Strange Nonchaotic Attractors

Article · February 1970

Source: CiteSeer

2 authors:

Awadhesh Prasad
University of Delhi

Ram Ramaswamy
Jawaharlal Nehru University

Strange Nonchaotic Attractors

Awadhesh Prasad*, Surendra Singh Negi, and Ramakrishna Ramaswamy

School of Physical Sciences

Jawaharlal Nehru University, New Delhi 110 067, INDIA

Abstract

Aperiodic dynamics which is nonchaotic is realized on Strange Nonchaotic attractors (SNAs). Such attractors are generic in quasiperiodically driven nonlinear systems, and like strange attractors, are geometrically fractal. The largest Lyapunov exponent is zero or negative: trajectories do not show exponential sensitivity to initial conditions. In recent years, SNAs have been seen in a number of diverse experimental situations ranging from quasiperiodically driven mechanical or electronic systems to plasma discharges. An important connection is the equivalence between a quasiperiodically driven system and the Schrödinger equation for a particle in a related quasiperiodic potential, giving a correspondence between the localized states of the quantum problem with SNAs in the related dynamical system. In this review we discuss the main conceptual issues in the study of SNAs, including the different bifurcations or routes for the creation of such attractors, the methods of characterization, and the nature of dynamical transitions in quasiperiodically forced systems. The variation of the Lyapunov exponent, and the qualitative and quantitative aspects of its local fluctuation properties, has emerged as an important means of studying fractal attractors, and this analysis finds useful application here. The ubiquity of such attractors, in conjunction with their several unusual properties, suggest novel applications.

*Present address: Department of Mathematics, Arizona State University, Tempe AZ 85287, USA

Contents

I. INTRODUCTION

One of the most enduring paradigms in the study of dissipative nonlinear dynamical systems has been the concept of a strange attractor. The term 'strange', introduced by Ruelle and Takens [1971], is used to describe a class of attractors on which the motion is chaotic, *i.e.*, showing exponential sensitivity to initial conditions [Eckmann and Ruelle, 1985]. Most known examples of strange attractors—the Lorenz attractor [Lorenz, 1963], for instance—also have fractal geometry, namely they are self–similar on different spatial scales, and further, are properly described by a spectrum of singular measures.

Grebogi, Ott, Pelikan, and Yorke [1984] constructed dynamical systems with attractors that were manifestly fractal, but on which the dynamics is *not* chaotic. The largest Lyapunov exponent, which is a measure of the rate of separation of trajectories with nearby initial conditions, is either zero or negative. At the same time, owing to the underlying fractal structure of the attractor, the dynamics is intrinsically *aperiodic*. These *Strange* (namely fractal) *Nonchaotic Attractors* (SNAs), which have been the focus of considerable interest from both theoretical and experimental points of view in the past few years, form the subject of this review.

Strange[1] nonchaotic attractors, although somewhat exotic, are not all that rare. They are *generic* in systems where there is quasiperiodic forcing, and are typically found in the neighborhood of related strange chaotic attractors in parameter space, as well as in the neighborhood of related periodic or quasiperiodic attractors. In a sense they represent dynamics which is intermediate between quasiperiodic and chaotic: there is no sensitive dependence on initial conditions, similar to motion on regular (periodic or quasiperiodic) attractors, but the motion is aperiodic, similar to dynamics on chaotic attractors.

---

[1] It should be pointed out that the originally intended meaning of the word strange in the definition of strange attractors was not restricted to the fractal geometric aspects alone; the strangeness was used to imply chaotic dynamics as well. The usage of the term in the context of SNAs refers to both the spatial fractal geometry and the temporal aperiodicity.

It is probably simplest to describe SNAs through an example. Consider the modified driven pendulum equation

$$\ddot{x} + \gamma\dot{x} = q_1 \sin\omega_1 t + q_2 \sin\omega_2 t - (x + \beta \sin 2\pi x) \tag{1}$$

which has been used to model a driven SQUID with inertia and damping [Zhou, Moss, and Bulsara, 1992]. For ω_1/ω_2 chosen to be an irrational ratio, the driving is quasiperiodic. Depending on the parameters β, γ, q_1 and q_2 , the attractors of this system, shown in Fig. 1 can be either strange and nonchaotic (Fig. 1(a)) or strange and chaotic (Fig. 1(b)).

Visually there is little to distinguish a SNA from a strange chaotic attractor since they superficially look very similar. Dynamically, though, there are important distinctions. This is most clearly evident in the behaviour of trajectories with nearby initial conditions, shown respectively in Figs. 1(c) and 1(d). Orbits converge and eventually coincide on the SNA, but on the chaotic attractor, they remain distinct and separate. Note that orbits on a chaotic attractor and on a SNA are both aperiodic. However, because the Lyapunov exponents are zero or negative on a SNA, trajectories do not separate from each other: thus SNA dynamics is in a sense predictable even though it is aperiodic. The property of robust synchronization is very characteristic of SNAs and can be utilized in a variety of applications which require aperiodicity [Ramaswamy, 1997].

Although the initial examples were constructed explicitly and could be considered as being somewhat artificial, SNAs are now known to be pertinent in a variety of physically relevant situations. The first experimental observation of a SNA was in a magnetoelastic ribbon [Ditto *et al.*, 1990]. This versatile mechanical system consists of a ribbon made of amorphous magnetostrictive material, which is clamped at the base and driven by an oscillating magnetic field. It has been extensively used to demonstrate and to implement a number of different ideas in the study of nonlinear dynamical systems. Quasiperiodic driving is achieved by using two oscillating magnetic fields with irrationally related frequencies, and the system is then modeled by a forced Duffing–like oscillator [Heagy and Ditto, 1991] with the equation of motion

$$\ddot{x} + \gamma\dot{x} = x\{1 + A[R\cos(t + \phi_0) + \cos\Omega t]\} - x^3. \tag{2}$$

where γ, A and R are parameters. If the frequency Ω is an irrational number, the system is quasiperiodically driven; in many cases, this number is chosen to be the golden mean ratio, $(\sqrt{5}-1)/2$. The sensitivity of this particular experiment was sufficient to verify the existence of SNAs from the data by estimating the fractal dimension of the underlying attractor and by observing power–law behaviour in the scaling of the spectral distribution (see Eq.(25) below).

SNAs can also be realized in electronic circuits, close to the transition to chaos [Yang and Bilimgut, 1997; Kapitaniak and Chua, 1997; Murali, Venkatesan and Lakshmanan, 1999]. In the typical case, a circuit is driven by two sinusoidal voltage sources with the frequencies irrationally related; the appropriate equations for the experiment of Yang and Bilimgut are (in standard notation)

$$\frac{dv_c}{dt} = \frac{1}{C}[i_L - \bar{g}(v_c)] \tag{3}$$
$$\frac{di_L}{dt} = \frac{1}{L}[Ri_L - v_c + f_1 sin(\omega_1 t) + f_2 sin(\omega_2 t), \tag{4}$$

Here f_1 and f_2 are the amplitudes and ω_1 and ω_2 are the frequencies of the two sinusoidal voltages. $\bar{g}(v_c)$, the nonlinear characteristic of the linear negative resistor, is given by $\bar{g}(v_c) = G_b v_1 + \frac{1}{2}(G_a - G_b)(|v_1 + E| - |v_1 - E|)$ and E is the breakpoint voltage.

An important area where the study of SNAs finds conceptual application is the case of quantum mechanical systems with quasiperiodic potentials. There is an unexpected link between wave–function localization phenomena and the related strange nonchaotic dynamics of an auxiliary variable, which was first pointed out by Bondeson *et al*. [1985] who considered the Schrödinger equation

$$-\frac{d^2\psi(x)}{dx^2} + \alpha V(x)\psi(x) = E\psi(x). \tag{5}$$

Defining $\phi(x)$ via the Prüfer transformation, namely $\exp i\phi(x) = (\psi' + ig\psi)/(\psi' - ig\psi)$, g being a constant, Eq. (5) can be brought into the form

$$\frac{d\phi}{dx} = \frac{1}{g}\{g^2 - [E - \alpha V(x)] \cos\phi + g^2 + [E - \alpha V(x)]\} \tag{6}$$

which is similar, for appropriate choice of potential $V(x)$ and suitable redefinition of the independent variable, to the forced pendulum system,

$$\dot{\phi} = \cos\phi + K + V_0(\cos\omega_1 t + \cos\omega_2 t). \tag{7}$$

It is known that SNAs exist in the above system if the frequencies ω_1 and ω_2 have an irrational ratio; upon varying K and V_0, SNAs can be observed in a finite interval in parameter space. The transformation connecting the two systems implies that quasiperiodic driving in the classical forced pendulum problem, Eq. (7) corresponds to a quasiperiodic potential in the isomorphic Schrödinger equation, Eq. (5).

In the quantum problem, which has been extensively studied, states can be localized or extended depending on whether α is relatively large or small. For the localized states, it happens that the inverse localization length is exactly the negative of the Lyapunov exponent of orbits in the corresponding classical problem [Bondeson *et al.*, 1985]: in this case, the localization length is positive, and therefore localized states of the quantum problem correspond to *attractors* in the dual (classical) dynamical system. Further analysis shows that these attractors have fractal geometry, thus giving the correspondence between SNAs and localized states.

Discretization of Eq. (5) permits further analysis. Ketoja and Satija [1997] have studied the Harper equation,

$$\psi_{k+1} - \psi_{k-1} + 2\alpha\cos 2\pi(k\omega + \theta_0)\psi_k = E\psi_k, \tag{8}$$

where k labels the sites of a 1–dimensional lattice, ψ_k is the wave function at the site and ω, θ_0 and α are parameters, while E is the energy eigenvalue. Upon transforming to the new variable $x_k = \psi_{k-1}/\psi_k$ (this is essentially the discrete version of the Prüfer transformation, cf. Eqs. (5-6) above), one obtains

$$x_{k+1} = \frac{-1}{x_k - E + 2\alpha\cos 2\pi\theta_k} \tag{9}$$

$$\theta_{k+1} = \theta_k + \omega \qquad \mod 1, \tag{10}$$

which, for irrational ω, is a quasiperiodically driven mapping that supports quasiperiodic, chaotic and strange nonchaotic attractors for different values of E and α. If $\alpha > 1$, eigenstates are exponentially localized, and correspond, as for the continuous system, to SNAs in Eq. (9-10) [Ketoja and Satija, 1997]. Furthermore, the absolute value of the Lyapunov exponent of the map in Eq. (9) is also the same as the inverse localization length in the Schrödinger problem if E happens to coincide with an eigenvalue. For $\alpha = 1$, states are still localized, but with power–law [André and Aubry, 1980] rather than exponential localization. Such states are termed *critical*, and the corresponding attractors in the classical map have all Lyapunov exponents equal to zero [Prasad *et al.*, 1999].

The study of SNAs thus clearly has relevance not only to dynamically important and unusual behaviour, but also to fundamental problems in other areas in physics.

In this review, we focus on a number of issues pertinent to the study of SNAs. Most known examples of systems with SNAs appear to have either quasiperiodic parametric modulation or quasiperiodic forcing, in the absence of which the systems support periodic or chaotic attractors. In Sec. II we discuss the general setting within which strange nonchaotic dynamics may be expected to occur, and the different techniques that have been used to characterize them. Some of the current interest in SNAs focuses on the question of "routes" or "scenarios" for their formation. This is both of theoretical interest, as a counterpoint to analogous routes or scenarios for the creation of chaotic attractors, as well as a practical question since experimental detection of SNAs can be facilitated if the mechanisms of creation of such behaviour are more clearly understood. Sec. III and IV are devoted to these aspects. In Sec. V, we discuss experimental observation of SNAs in diverse physical systems, and their possible applications. The review concludes with a summary in Sec. VI.

II. STRANGE NONCHAOTIC DYNAMICS: OCCURRENCE AND CHARACTERIZATION

There are two issues that need to be satisfactorily resolved for the study of SNAs in a dynamical system. The first is to establish the strangeness of the attractor and its nonchaotic nature without recourse to numerical estimates of either the fractal dimension or the Lyapunov exponents. The second is to establish that SNAs occur in a finite interval in parameter space, and not just at isolated points, in which case they would merely be mathematical curiosities which would be difficult to observe in practice. In general these issues are not easily settled, but for particular systems some results have been obtained [Brindley and Kapitaniak, 1991; Keller, 1996; Bezhaeva and Oseledets, 1996].

A driven dynamical system is usually described through equations of motion such as Eqs. (1) and (2) above, or as a set of coupled ordinary differential equations,

$$\dot{\mathbf{X}} = \mathbf{F}(\mathbf{X}, \mathbf{t}). \tag{11}$$

Through standard procedures, say by projecting the motion onto a lower dimensional subspace, or by sampling the variables stroboscopically, the above continuous time dynamical system can be reduced to a discrete mapping (see for example, Ott [1994]). It is sometimes preferable to study discrete mappings since these capture the essential features of the dynamics and can be mathematically easier to analyse.

Most of the quasiperiodically driven systems where SNAs have been studied are skew–product dynamical mappings of the general form

$$\mathbf{X_{n+1}} = \mathbf{F}(\mathbf{X_n}, \theta_\mathbf{n}) \tag{12}$$

where $\mathbf{X} \in \mathbf{R^k}$ is a k-dimensional vector and $\theta \in \mathrm{S}^1$ is a scalar which varies quasiperiodically. The simplest (but not the only) way in which this is accomplished is via the rotation,

$$\theta_{n+1} = \theta_n + \omega \bmod 1, \tag{13}$$

since if ω is an irrational number, then successive iterates of θ will densely and uniformly cover the unit interval in a quasiperiodic manner. The parameters of the mapping $\mathbf{F}$ are modulated via θ (see the examples below), resulting in a quasiperiodically driven dynamical system. A particular case that has been extensively studied is the driven 1–dimensional logistic map [Heagy and Hammel, 1994], namely

$$x_{n+1} \equiv F_{\alpha,\epsilon}(x_n, \theta_n) = \alpha[1 + \epsilon\cos(2\pi\theta_n)]x_n(1 - x_n), \tag{14}$$

with ω usually taken to be the golden mean ratio. The phase–diagram for this system which details the different dynamical states that are obtained as a function of the parameters α and ϵ has been extensively studied [Prasad *et al.*, 1997, 1998; Witt *et al.*, 1997] and is shown in

Fig. 2. SNAs occur in several different parameter ranges, between regions of periodic or torus attractors and regions of chaotic attractors. Indeed, the dynamics in the transition region between regular and chaotic motion is quite complicated, and the boundaries separating different types of attractors are very convoluted.

The system first considered by Grebogi, Ott, Pelikan, and Yorke [1984] is a similar mapping with (cf. Eq. (12))

$$F_\alpha(X_n, \theta_n) \equiv 2\alpha \cos 2\pi\theta_n \tanh x_n. \tag{15}$$

The following arguments [Grebogi *et al.*, 1984] establish the existence of SNAs for appropriate values of α.

- In the absence of the quasiperiodic driving, the mapping $x_{n+1} = 2\alpha \tanh x_n$ is 1–1 and contracting, mapping the real line into the interval $[-2\alpha, 2\alpha]$. Because ω is an irrational number, the dynamics in θ [cf. Eq. (13)] is ergodic in the unit interval. The attractor of the dynamical system Eq. (15) therefore must be contained in the strip $[-2\alpha, 2\alpha] \otimes [0, 1]$.

- A point x_n with the corresponding $\theta_n = 1/4$ will map to $(x_{n+1} = 0, \theta_{n+1} = \omega + 1/4)$, after which subsequent iterates will all remain on the line $(x = 0, \theta)$. The same holds for points with $\theta_n = 3/4$. This line therefore forms an invariant subspace: an orbit starting on $(x = 0, \theta)$ will stay on it.

- However, as can be seen by taking the derivative of F, the dynamics on this line is *unstable* if $|\alpha| > 1$ (the Lyapunov exponent, defined below, can be computed exactly within the invariant subspace, and happens to be $\log|\alpha|$). Thus, it follows that the attractor has a dense set of points on the line $x = 0, \theta \in [0, 1]$ (since ω is irrational), but the entire line itself cannot be the attractor for $\alpha > 1$, since the dynamics is unstable on that line.

- The attractor therefore must have an infinite set of discontinuities and therefore, a fractal structure. An explicit (numerical) computation for particular values of $|\alpha| >$

1 yields a negative value for the nonzero Lyapunov exponent, confirming that the attractor is both strange and nonchaotic.

Bezhaeva and Oseledets [1996] have rigorously shown for this system that for any irrational ω and for α sufficiently large, a SNA with a singular–continuous spectrum exists. Stronger results which can be obtained [Keller, 1996] confirm that the attractor is a fractal and is the topological support of an ergodic SRB (Sinai–Bowen–Ruelle) measure. Eckmann and Ruelle [1985] discuss the utility of such measures for fractal attractors on which the invariant measure is spatially nonuniform.

Another class of systems where some analytical results are possible are the strange attractors of the Harper equation. Given the correspondence between the dynamical system and the quantum problem, it is possible to establish the existence of attractors with a negative Lyapunov exponent and a fractal structure [Ketoja and Satija, 1997; Prasad *et al.*, 1999]. Mathematically rigorous results are more difficult in this case, but there is some indication that it will be possible to have fractal nonchaotic attractors in a large class of systems, even in the absence of explicit quasiperiodic driving [Negi and Ramaswamy, 2000a].

Most studies of SNAs to date have made recourse to heuristic arguments and "experimental" verifications, through explicit computation of the Lyapunov exponents and fractal dimensions. A number of different quantitative methods have been introduced over the past several years that have proven useful in verifying the strangeness of these nonchaotic attractors.

A. Lyapunov exponents and Fractal Dimensions:

For a dynamical system of the form of Eq.(12), there are k nontrivial Lyapunov exponents $\Lambda^m, m = 1, 2, \ldots, k$. These characterize the manner in which a k–dimensional parallelepiped evolves under the dynamics in the phase space, and are obtained by examining the rate of stretching of vectors tangential to the flow. The Lyapunov exponent corresponding to the θ freedom where the flow is uniform has the value zero.

To compute the Lyapunov exponent it is necessary to propagate k-dimensional orthonormal vectors, $\hat{\mathbf{e}}^m, m = 1, \ldots, k$ in the tangent space, namely according to the dynamics

$$\mathbf{e}_j^m = \mathbf{JF}(\mathbf{X_j}, \theta_\mathbf{j}) \ \cdot \hat{\mathbf{e}}^\mathbf{m}_\mathbf{j-1} \tag{16}$$

where $\mathbf{JF}(\mathbf{X}, \theta)$ is the Jacobian matrix of $\mathbf{F}$ along the orbit and the subscript j refers to the time step. At each step along the trajectory, the vectors $\mathbf{e}_j^m$ are reorthogonalized, and the norms give the expansion (or contraction) along the different directions in phase space [Benettin, Galgani and Strelcyn, 1976]. From this it is possible to compute the spectrum of Lyapunov exponents as

$$\Lambda^m = \lim_{N \to \infty} \frac{1}{N} \sum_{j=1}^{N} \ln \|\mathbf{e}_j^m\|, \qquad m = 1, 2, \ldots k. \tag{17}$$

The quantity $\ln \|\mathbf{e}_j^m\| \equiv y_j^m$ is the "stretch–exponent": this measures the expansion (or contraction) factor at step j in the mth direction. One can further define local, N–step, or finite–time Lyapunov exponents as

$$\lambda_N^m = \frac{1}{N} \sum_{j=1}^{N} y_j^m, \qquad m = 1, 2, \ldots k; \tag{18}$$

examining the distribution of these quantities has proven useful in the study of fractal attractors (see below).

Most studies have focused on the largest of the Lyapunov exponents, Λ^1, which is of most importance in determining the dynamics; the superscript will henceforth be omitted. This is not to suggest that the other Lyapunov exponents are unimportant: indeed, in higher dimensional systems with so–called unstable dimensional variability [Dawson *et al.*, 1994; Kostelich *et al.*, 1997] the higher Lyapunov exponents, Λ^2, etc. play a major role. (For dynamical systems described by a set of coupled differential equations, Lyapunov spectra and finite time Lyapunov exponents can be similarly defined.)

A number of reliable methods are available for the computation of the asymptotic Lyapunov exponents [Bennettin, Galgani, and Strelcyn, 1976; Eckmann and Ruelle, 1985], although for experimental data, when working with a single time series, even this can be a problem since it is often difficult to reliably compute a small negative Lyapunov exponent using standard algorithms [Wolf *et al.*, 1985]. The effect of noise within experimental data can be removed to some extent by filtering techniques, and recently developed methods have made it possible to extract negative Lyapunov exponents from model and experimental data with some degree of success [Huang *et al.*, 1994].

Although the largest Lyapunov exponent is negative on SNAs, owing to the strangeness of the attractor, the dynamics can be *locally* unstable. The negative Lyapunov exponent arises from the fact that these instabilities are compensated by regions where the dynamics is locally stable. Such effects are best explored by the examination of the distribution of the finite–time Lyapunov exponents [Grassberger *et al.*, 1988; Abarbanel *et al.*, 1991] defined in Eq. (18). The stationary density of finite–time Lyapunov exponents is

$$P(N,\lambda)d\lambda \equiv \text{ Probability that } \lambda_N \text{ takes a value between } \lambda \text{ and } \lambda + d\lambda, \tag{19}$$

and this can be obtained by taking a long trajectory, dividing it in segments of length N, and calculating λ_N in each segment. Since $\lim_{N\to\infty} P(N,\lambda) \to \delta(\Lambda - \lambda)$, for finite N the density is usually peaked around the asymptotic Lyapunov exponent, and has a characteristic shape and width [Prasad and Ramaswamy, 1999]. Several studies [Pikovsky and Feudel, 1995; Prasad and Ramaswamy, 1998 and 1999] have established that for SNAs the local instability results in the density of local Lyapunov exponents having some component at positive λ; this component decreases with N, and can be used to characterize SNAs. An example of such a density is shown in Fig. 3 for a SNA in the forced logistic map; Λ is negative, but even for long stretches of any trajectory—the time interval $N = 1000$ in this instance—the dynamics can be unstable, giving a positive local Lyapunov exponent. This feature distinguishes SNAs from other (periodic or quasiperiodic) nonchaotic attractors.

The fractality of the attractor cannot be as easily determined through computation of the fractal dimensions such as the capacity (D_0) and information (D_1) dimensions using standard algorithms [Ding *et al.*, 1989]. The Kaplan–Yorke conjecture [Kaplan and Yorke, 1979] for the Lyapunov dimension D_L, if expected to be valid even in this situation, gives the estimate $D_L = D_1 = 1$; this distinguishes SNAs from very similar chaotic attractors wherein

D_1 would be expected to be larger than 1. Because of conflicting local and global stability features on SNAs, numerical results are not always conclusive: an inordinately large number of points is needed to get converged exponents for fractal dimensions [Ding *et al.*, 1989].

Although the criteria discussed above, based on the behaviour of Lyapunov exponents and fractal dimensions, are essential to a mathematical characterization of SNAs, other measures are needed, particularly for examining numerical or experimental data. We discuss some of these next.

B. Phase and Parameter Sensitivity:

If the attractor $x(\theta)$ is viewed as a fractal curve, then its non differentiability can be detected by examining the separation of points that are initially close in θ. Pikovsky and Feudel [1995] introduced a measure to characterize strangeness by calculating the derivative $dx/d\theta$ along an orbit, and finding its maximal value. This yields the phase sensitivity function

$$\Gamma_N = \min_{x,\theta}[\max_{1<N}|dx_N/d\theta|], \tag{20}$$

as the smallest such realization for arbitrary (x, θ), so that a bound can be set on the rate of growth of Γ over the entire attractor. For a chaotic attractor, the sensitivity grows exponentially while for a SNA, Γ_N (shown in Fig. 4) grows as a power,

$$\Gamma_N \propto N^{\mu}, \tag{21}$$

with μ typically > 1 [Nishikawa and Kaneko, 1996; Pikovsky and Feudel, 1995]. Other similar measures can also be devised to distinguish between strange and non–strange attractors. For example, if one computes the integral of the derivative $dx_N/d\theta$ as a function of θ: for a smooth curve, this integral converges, whereas if there are an infinite number of discontinuities in $x(\theta)$ as for a fractal, it diverges.

The phase sensitivity seems to be a robust method for determining the fractality of the attractor [Pikovsky and Feudel, 1995]; this method can be directly generalized to higher dimensional systems as well [Sosnovtseva *et al.*, 1996]. Sensitivity to a parameter, say to the amplitude of the driving term can be analogously defined [Nishikawa and Kaneko, 1996], as

$$\Gamma_N^\epsilon = \min_{x,\theta}[\max_{1<N}|dx_N/d\epsilon|], \tag{22}$$

and this quantity also shows a power–law dependence on N.

C. Correlations and Power spectra:

Pikovsky *et al.*[1995] considered the averaged squared autocorrelation function as a means of distinguishing SNA dynamics from chaotic motion. The autocorrelation function for the dynamical variable is defined in the usual manner, namely

$$C(\tau) = \frac{< x_i x_{i+\tau} > - < x_i >< x_{i+\tau} >}{< x_i^2 > - < x_i >^2} \tag{23}$$

where i is a discrete time index, $\tau = 0, 1, \ldots$ is the time shift, and $<>$ denotes a time–average. For periodic motion

$$C_{av}(t) = \frac{1}{t}\sum_{\tau=0}^{t-1}|C(t)|^2, \tag{24}$$

the average squared autocorrelation asymptotes to 1 ($C(\tau)$ oscillates between 0 and 1). Since quasiperiodic motion does not recur exactly, for such dynamics the average asymptotes to a value less than 1. For chaotic motion, C_{av} decreases exponentially to 0, while for the case of SNAs the behaviour is intermediate.

More quantitative distinctions come from studies of the discrete Fourier transform of the time series $\{x\}$ generated by the dynamical equation. The number of peaks in the transform,

$$T_k = \sum_{m=1}^{N} x_m \exp(-i2\pi mk/N), \quad k = 0, \ldots, N \tag{25}$$

above a threshold σ shows the scaling $\mathcal{N}(\sigma) \sim \sigma^\alpha$, where the exponent α is between 1 and 2 if the attractor is strange. This measure can be used to distinguish SNA dynamics from other nonchaotic behaviour: for motion on an $(n-1)$–frequency quasiperiodic attractor the variation is $\mathcal{N}(\sigma) \sim (1/\log\sigma)^{n-1}$ [Romeiras *et al.*, 1987].

Other transforms have also been used, as for example the partial Fourier sums,

$$T(\Omega, N) = \sum_{k=1}^{N} x_k \exp(i2\pi k\Omega), \tag{26}$$

where Ω is proportional to the irrational driving frequency ω [Pikovsky *et al.*, 1995; Yalçinkaya and Lai, 1997]. The graph of Re T vs. Im T is a curve on the plane which may be treated as a "walk", and one can compute the mean square displacement $|T(\Omega, N)|^2$. If the "walk" is Brownian, then $|T(\Omega, N)|^2 \sim N$, and the spectrum is continuous, while if $|T(\Omega, N)|^2 \sim N^2$, there is a discrete spectral component at frequency Ω. SNAs, in contrast, have a singular–continuous spectrum, which implies the scaling $|T(\Omega, N)|^2 \sim N^\beta$ with $1 < \beta < 2$ (see Fig. 5).

III. SCENARIOS FOR THE FORMATION OF SNAS

In the absence of quasiperiodic forcing, a dissipative nonlinear dynamical system typically has periodic attractors or chaotic attractors. With the introduction of quasiperiodic driving, as for example in the mapping in Eq. (12) or the flows in Eqs. (1-2), periodic attractors become quasiperiodic attractors: the motion lies on tori in the phase space, and these are characterized by the number of independent frequencies contributing to the quasiperiodicity. When the parameter itself is further varied, quasiperiodic or chaotic attractors can become SNAs.

Exactly what constitutes a distinct route or mechanism for the formation of a strange nonchaotic attractor is somewhat nebulous since the bifurcations of quasiperiodically driven systems have not been studied in detail. However, several routes to SNAs have been described in the literature and there are parallels with the different scenarios through which chaotic attractors are created [Eckmann, 1981; Ott, 1994]. In the next Sec. we will examine the variation of the Lyapunov exponent (and its variance) as the control parameter is varied. Several studies have established that the different scenarios have distinctive signatures [Prasad *et al.*, 1998]. For that purpose, it is helpful to first describe these bifurcations by discussing the dynamics as a function of a control parameter for several known scenarios for the formation of SNAs. These are depicted in Fig. 6, where the torus (before the bifurcation) and the SNA (after the bifurcation) are shown.

A. Torus Collisions:

One situation wherein the bifurcation is well studied is the mechanism for SNA formation via torus collisions.

A period–doubling bifurcation in a quasiperiodically driven system gives rise to a stable doubled torus, with the parent torus becoming unstable. (Without driving, this is just the pitchfork bifurcation [Ott, 1994], a period 2^n orbit becomes unstable and bifurcates to a period 2^{n+1} orbit.)

Heagy and Hammel [1994] identified the birth of a SNA with the collision between the doubled quasiperiodic torus and its unstable parent. This requires first that a period–doubling bifurcation occur, after which the stable torus attractor gets progressively more "wrinkled" as the parameters in the system change, i.e., $\mathbf{X}(\theta)$ becomes more and more oscillatory as in Fig. 6(a). Concurrently, the unstable parent torus also gets more oscillatory. At an analogue of the attractor–merging crisis that occurs in chaotic systems [Grebogi *et al.*, 1987], the SNA is created at the collision of the period–doubled torus and its unstable parent as in Fig. 6(b), the Lyapunov exponent remaining negative throughout this crisis.

This route has been seen in a number of different systems, most notably in the quasiperiodically forced logistic map, Eq. (14), which has been extensively studied [Heagy and Hammel, 1994; Prasad *et al.*, 1998]. Feudel, Kurths, and Pikovsky [1995] have also identified other torus collision mechanisms that are operative in forced circle maps, where a stable and unstable torus intersect on a dense set of points to give a SNA. A torus collision is thus a general feature of forced systems and is a common mechanism for SNA creation.

B. Fractalization:

In the "fractalization" route for the creation of SNAs [Kaneko, 1984; Nishikawa and Kaneko, 1996] a quasiperiodic torus gets increasingly wrinkled and transforms into a SNA without the apparent mediation of any nearby unstable periodic orbit. Fractalization is also a likely cause for the interruption of the cascade of torus doublings [Kaneko, 1984]. It appears unlikely that there is an explicit bifurcation that is involved in this scenario, but in some sense this is the most general route to SNA that is observed in driven systems; Fig. 6(c,d) shows a torus and its fractalized SNA across the transition.

C. Intermittency:

The intermittency scenario for the formation of SNAs [Prasad *et al.*, 1997; Witt *et al.*, 1997] is as follows. Upon varying a parameter, a chaotic strange attractor is first transformed into a SNA (see Fig. 6(e,f)) which is then eventually replaced by a one-frequency torus through an analogue of the saddle–node bifurcation. By varying the parameter one can traverse the transition in the opposite direction, so the defining characteristic of the bifurcation is the abrupt change of a torus to a SNA, as will be discussed in detail in the next Sec.

The intermittent dynamics at this bifurcation are of Type I [Pomeau and Manneville, 1980]. Since the SNA occupies a much larger portion of the phase space as compared to the torus from which it originated, this transition shares some of the features of a widening crisis in unforced systems [Grebogi *et al.*,1987; Mehra and Ramaswamy, 1996]. The discontinuous change of Λ at a saddle–node bifurcation is softened by the quasiperiodic forcing, and for $\alpha < \alpha_c$, the Lyapunov exponent shows the scaling [Prasad *et al.*, 1997]

$$\Lambda - \Lambda_c \sim (\alpha_c - \alpha)^{\mu}. \tag{27}$$

This route to SNA is quite general (this was termed Route C by Witt, Feudel and Pikovsky, [1997]), and has been seen in a number of driven maps and in flows, such as the forced Duffing equation, as well [Venkatesan *et al.*, 1999].

D. The Blowout bifurcation:

In systems with a symmetric low–dimensional invariant subspace containing a quasiperiodic torus, a blowout bifurcation [Ott and Sommerer, 1994] leads to the formation of a SNA [Yalçinkaya and Lai, 1996].

Trajectories starting in the invariant subspace, $\mathcal{S}$, remain in $\mathcal{S}$. The Lyapunov exponent Λ has two components, one of which, Λ_T, is defined for trajectories in $\mathcal{S}$ with respect to perturbations in a transverse subspace $\mathcal{T}$. A positive Λ_T indicates that trajectories in the vicinity of $\mathcal{S}$ are repelled away from it, and this gives rise to strangeness. At the blowout bifurcation, Λ_T changes its sign, becoming positive as a system parameter varies. If, concurrently, $\Lambda < 0$, the attractor is a SNA.

Yalçinkaya and Lai [1996] studied a number of systems wherein the blowout bifurcation occurs, including the mapping

$$F_{a,b}(x_n, \theta_n) = (\alpha \cos 2\pi\theta_n + b) \sin 2\pi x_n \tag{28}$$

and showed the presence of SNAs in a range of parameter values when $\Lambda_T > 0$ and $\Lambda < 0$. The quasiperiodic torus and the corresponding SNA after the bifurcation are shown in Fig. 6(g,h). This route is found only in those situations where an invariant subspace exists. Although it does not occur, for example, in the driven logistic map, Eq. (14), this scenario is quite general and has been seen in a continuous dynamical system similar to Eq. (1). The system where SNAs were first discovered, namely Eq. (15) is also of this type, the invariant subspace being the line $x = 0$.

E. Quasiperiodic Routes:

Other than the above four principal scenarios, a number of different quasiperiodic routes to SNAs have been discussed in the literature. These scenarios appear in systems wherein the (unforced) dynamics itself shows quasiperiodicity, as for example the forced circle map, where

$$F_{K,V,\epsilon}(x_n, \theta_n) = x_n + 2\pi K + V \sin x_n + \epsilon \cos \theta_n, \tag{29}$$

K, V being parameters, and ϵ being the forcing amplitude [Ding *et al.*, 1989]. These routes are more descriptive of the different dynamical states that the system passes through (say from an n–frequency quasiperiodic torus attractor to a SNA) than of distinctive bifurcation routes: one finds that the actual transition to SNAs is through the mechanisms discussed above. The torus collision scenario is operative in slightly different form here as well [Feudel *et al.*, 1995], the collision here is between a stable and unstable torus at a dense set of points. We have also found that the fractalization route also operates in the same regions. Since there is an immense variety in the different types of periodic, quasiperiodic and chaotic dynamical states that are possible in nonlinear systems, there are likely to be several such states as precursors to the eventual SNA [Venkatesan and Lakshmanan, 1998].

F. Homoclinic Collision:

An important class of bifurcations which are peculiar to driven maps of Harper type, namely Eq. (9) and its generalizations [Negi and Ramaswamy, 2000b] are homoclinic collisions leading to the formation of SNAs [Prasad *et al.*, 1999]. Below the transition, the dynamics is on invariant curves with a finite number of branches, see Fig. 6(i). As the parameter is increased, these branches approach each other (the distance between branches decreases as a power in the effective parameter), eventually colliding at a dense set of points and forming an SNA (Fig. 6(j)). It can be shown that the collision of the invariant curve with itself is accompanied by an unusual "symmetry–breaking" [Prasad *et al.*, 1999] which also help to establish the non-positivity of the Lyapunov exponent on the SNA.

IV. DYNAMICAL TRANSITIONS

The strange nonchaotic state is dynamically distinct from the strange chaotic state, and morphologically distinct from the quasiperiodic (and nonchaotic) torus attractor. The transitions between these different states as a parameter is varied are quite distinctive, and have been the focus of considerable interest. In addition to the scenarios for the creation of SNAs discussed in the previous section, there can be other bifurcations and crises in these systems.

The Lyapunov exponent is a good order parameter to study these dynamical transitions. Further, since the attractor changes drastically at the transition, the variance of the distribution of finite–time Lyapunov exponents, Eq. (19), are also known [Prasad *et al.*, 1998] to provide a good order parameter whereby the studied.

The different scenarios for the formation of SNAs all have characteristic signatures in the manner in which the exponent changes at the transition, and in the manner in which the variance changes at the transition. Figure 7 shows the behaviour of these quantities for the bifurcations discussed in Sec. III.

When the transition occurs via torus collisions (the Heagy–Hammel mechanism, for instance), the Lyapunov exponent typically shows a point of inflexion while the variance increases (see Fig. 7(a,b)). In the fractalized route there is no apparent crisis involved, and therefore the Lyapunov exponent and variance increase only slowly as shown in Fig. 7(c,d). At the saddle–node bifurcation leading to the intermittent SNA, the Lyapunov exponent shows an abrupt change, with a power–law (Eq. (27)) dependence on the parameter on the SNA side of the transition (see Fig. 7(e,f)). The fluctuations in the Lyapunov exponent (determined, e. g., from considering a large number of trajectories) shows a remarkable and abrupt increase at the transition. For the blowout bifurcation, the behaviour of the Lyapunov exponent is distinctive. Below the transition, both Λ and the transverse exponent Λ_T (see the discussion in Sec. III) are identical and negative. As the parameter a in Eq. (28) is varied, they increase and become zero at the critical value, a_c. After the bifurcation, Λ is negative, but Λ_T is positive, leading to locally unstable motion with a corresponding increase in the fluctuations of the Lyapunov exponent across the transition; see Fig. 7(g,h). Recent analysis of finite–time Lyapunov exponents at this bifurcation has shown that there is a symmetry–breaking that accompanies the transition to SNAs [Prasad *et al.*, 1999]. In the homoclinic transition to SNAs which occurs in maps of Harper type, the Lyapunov exponent changes from zero to a negative value. At the transition, the exponent converges as a power–law rather than exponentially: these SNAs are critical [Negi and Ramaswamy, 2000c]. The fluctuations increase across the transition as may be expected from general considerations, but this is not easy to distinguish numerically owing to the slow convergence of quantities in the neighborhood of the transition. Thus the counterparts of Figs. 6(i) and (j) are not very instructive.

In most systems where there are SNAs, there are a large number of different dynamical states that are possible and therefore a large number of different dynamical transitions that can occur. For SNA $\rightarrow$ SNA transitions, as has been described and characterized in the literature, the Lyapunov exponent is a good order parameter. One situation where this is *not* so is the SNA $\rightarrow$ chaotic attractor transition. The transition is not accompanied by any major change in the form or shape of the attractor, and the Lyapunov exponent itself changes only from being negative to positive, passing *linearly* through zero [Lai, 1996] (see Fig. 8(a)). However, the fluctuations on the attractor seem to increase substantially, with the variance of the distribution showing a small but noticeable increase across the transition (Fig. 8(b)).

Symmetry Breaking

Several bifurcations in dynamical systems are distinguished by the fact that the Lyapunov exponent passes through zero: common examples are the pitchfork and tangent bifurcations in the absence of driving, when the slope of the map takes (absolute) value 1 (see for example, Ott [1994]).

With driving, the scenarios for the transition to SNA are, as discussed in the previous section, analogus to bifurcations leading to chaotic states, although the Lyapunov exponent typically does not pass through the value zero (since it is nonpositive through the transition). In two of the scenarios, however, it does: these are the blowout bifurcation route [Yalçinkaya and Lai, 1996], and in the case of homoclinic collisions leading to SNA [Prasad *et al.*, 1999].

These transitions are accompanied by a novel symmetry breaking. The Lyapunov exponent, Λ measures the average expansion rate along a trajectory,

$$\Lambda = \lim_{N \to \infty} \frac{1}{N} \sum_{j=1}^{N} y_j, \tag{30}$$

the y's being the stretch–exponents in the principal direction (namely $m = 1$ in Eq. (17)). The stretch exponents are different at each point of the orbit (since there are no periodic orbits in such systems). In the sum above, there are several ways in which the Lyapunov exponent can become zero, but it turns out that at the blowout bifurcation, there is an exact quasiperiodic symmetry in the stretch exponents. This can be seen by plotting y_j versus

y_{j+1}, the return map for stretch exponents as in Fig. 9(a), where the symmetry with respect to the diagonal is clearly evident. This holds exactly at the bifurcation point here as well as in the case of homoclinic collisions in the Harper map [Prasad *et al.*, 1999]. When the symmetry is broken, the total Lyapunov exponent becomes negative and the dynamics is on a SNA: see Fig. 9(b).

There are other possibilities that will result in a zero Lyapunov exponent. The symmetries may be more complex [Prasad *et al.*, 2000], for instance, or there may be no symmetries at all, as in the SNA $\rightarrow$ chaos transition [Negi *et al.*, 2000].

V. EXPERIMENTS AND APPLICATIONS

Given the ubiquity of SNA dynamics in quasiperiodically driven systems, one of the main issues with respect to the experimental observation of SNAs is whether such attractors are robust to noise.

It is known [Crutchfield, Farmer and Huberman, 1982] that noise generally lowers the threshold for chaos: systems with additive noise have a *larger* Lyapunov exponent for smaller nonlinearity. However, the effect of noise depends on the nature of the system (see e. g., Schroer *et al.*[1998] and references therein, and Prasad and Ramaswamy [2000]). Quasiperiodically driven systems also show an enhancement in the Lyapunov exponent, but depending on the system, Λ in the presence of noise can still be negative, and the SNAs can continue to exist [Prasad, Mehra and Ramaswamy, 1998]. The addition of noise usually "smears out" the attractors, and the threshold values for bifurcations typically shift to lower parameter values, but the actual transitions—now from noisy tori to noisy SNAs—survive.

A number of different experiments have verified the existence of SNAs, ranging from driven mechanical systems such as the magnetoelastic ribbon experiment [Ditto *et al.*, 1990] to electronic circuits. Zhou *et al.*[1992] studied the model SQUID system, Eq. (1) above, on an analog simulator, and verified SNA dynamics by computing power spectra and Lyapunov experiments. Similar experiments have been implemented in the forced Ueda's circuit [Liu and Zhu, 1996], the forced Chua's circuit [Zhu and Liu, 1997] and the forced Murali–

Lakshmanan–Chua circuit [Yang and Bilimgut, 1997].

It should be noted that for the experimental characterization of SNAs, there are practical problems and limitations. Lyapunov exponents can be estimated from experimental data, but the inherent noise can make it very difficult to determine a small negative exponent. The error bounds obtained by application of standard algorithms can be large enough to make estimates inconclusive. The same holds for fractal dimension estimates.

Experimentally, the spectral distribution function measure discussed in Sec. 2 has been used in addition to the Lyapunov exponent or the fractal dimension obtained from analysis of time series data. In most cases, the scaling behaviour of this function is more unambiguous than other measures.

Plasma systems have also been extensively used in order to study a number of nonlinear dynamical effects, and in recent measurements of the glow discharge in a neon gas plasma [Ding *et al.*, 1997], SNAs have been observed in the absence of any driving. The quasiperiodic driving comes from autoexcitations of the plasma, and the nature of the attractor was verified through dimension and Lyapunov exponent estimations. Another SNA system where there is no explicit external forcing is the model study of a neuronal membrane system as well as the EEG data examined by Mandell and Selz [1993], but the origin of the quasiperiodic driving there is less clear.

One property of SNAs that make them interesting experimental systems for study—from the viewpoint of potential applications—is their relative ease of synchronization. In recent years the synchronization and control of chaotic systems has been the focus of much research activity [Shinbrot, 1995; Chen and Dong, 1998]. Two identical nonlinear chaotic dynamical systems can be made to synchronize by using one (the *drive*) to drive the other (the *response*). Pecora and Carroll [1990] showed that if the Lyapunov exponents corresponding to the response subsytem were negative, then synchronization would occur.

Such synchronization is trivially achieved with SNAs since the largest Lyapunov exponent is already negative. Further, even coupling the systems is unnecessary so long as the initial phases are matched, again because of the negative Lyapunov exponents [Ramaswamy, 1997]; see Fig. 1(c) for an illustration.

In juxtaposition with the fact that the dynamics on SNAs is aperiodic, this gives rise to interesting possibilities for their use. Two recent proposals outline the use of SNAs in the area of secure communications. Zhou and Chen [1997] transmit digital information by modulation of a system parameter so that the dynamics switches between a SNA and another chaotic or nonchaotic attractor. Information is recovered at the receiver by employing the synchronization between the nonchaotic attractor of the receiver and the transmitter. Another implementation [Ramaswamy, 1997] uses two identical independent SNAs which are synchronized by in-phase driving but are otherwise uncoupled. The principle employed is similar to that of chaotic masking. A low–amplitude information signal is added to the output of the transmitter SNA system. Since the SNA dynamics is aperiodic, the resulting signal also aperiodic. The receiver SNA system is exactly synchronized with the transmitter, and thus the information can be simply recovered by subtracting the two signals (see Fig. 3 in Ramaswamy, [1997]).

VI. SUMMARY

Strange nonchaotic attractors are an important class of dynamical attractors that are generic in quasiperiodically driven nonlinear dynamical systems, both mappings as well as flows. Systems where SNAs arise naturally span a wide range since the possibility of such dynamics devolves on a combination of dissipation, nonlinearity and quasiperiodic modulation.

The skew–product structure (whereby the "system" dynamics does not feed into the dynamics of the forcing term) is common to all examples of systems with SNAs that have been studied so far. Furthermore, explicit quasiperiodic driving is also a feature of hitherto studied systems. However, both these features are probably not necessary in order that SNAs be formed [Negi and Ramaswamy, 2000a]. In particular, driving a system with signals based on fractal sequences also appears to yield SNAs [Kuptsov, 1998].

Very recently Cassol, Veiga and Tragtenberg [Cassol *et al.*, 2000] have studied a map with *periodic* forcing, where they find apparent strange nonchaotic motion with Lyapunov exponent equal to zero, and orbits on a fractal attractor. No other examples of periodically driven systems with SNAs are known so far, and from general considerations, it would appear unlikely that such attractors can occur under conditions of periodic forcing. Anishchenko *et al.*[1996] reported the presence of a SNA in a periodically forced system, but this result has been questioned [Pikovsky and Feudel, 1997]. We have also examined this system and find only chaotic and periodic attractors.

Modulation of chaotic systems can lower the Lyapunov exponent by enhancing the measure on contracting regions of phase space. This means of "control" can sometimes create SNAs if the exponent is sufficiently lowered, as discussed recently [Shuai and Wong, 1998, 1999]. For the case of chaotic or noisy driving, Rajasekhar [1995] has shown the possibility of nonchaotic dynamics via a type of chaos control, but this methodology does not necessarily lead to attractors [Prasad and Ramaswamy, 2000]. The question of whether there can be SNAs with other types of forcing remains open.

In this review, we have described the general phenomenology of such systems, with particular emphasis on the scenarios for the creation of SNAs. We have also described the many different methods that have been employed to confirm strange nonchaoticity. SNAs are relevant in a number of theoretical and experimental situations, and these have been discussed in some detail. One of the other principal themes in current research is the use of the Lyapunov exponent and its fluctuations as order–parameters for characterizing and determining different dynamical transitions in these systems. Both the exponent as well as the fluctuations show characteristic variation with system parameters, and this is as true of transitions from tori to SNAs as it is for transitions from SNAs to SNAs, or from SNAs to chaotic attractors.

Applications and experiments that exploit the unusual properties of SNAs are beginning to be devised. Much of our discussion has centered around the dynamics of low–dimensional systems since these are simple enough to analyse and most of the concepts and phenomena in the study of SNAs can be illustrated here. Extensions to higher dimensions of many of the phenomena and arguments are straightforward, and have begun to be explored in the literature.

ACKNOWLEDGMENT

We are grateful to Mike Cross and Jim Heagy for discussions and for their comments on an earlier version of this manuscript. We would also like to thank Jim Heagy for sharing his code for locating unstable tori, and M Lakshmanan and A Venkatesan and Vishal Mehra for discussions on SNAs. This work was supported by a grant from the Department of Science and Technology, India.

REFERENCES

Abarbanel, H. D. I., Brown, R. & Kennel, M. B. [1991] "Local Lyapunov exponents computed from observed data," *J. Nonlinear Sci.* **2** ,343–365.

Anishchenko, V. S., Vadivasova, T. E. & Sosnovtseva, O. [1996] "Strange nonchaotic attractors in autonomous and periodically driven systems," *Phys. Rev. E* **54**, 3231–3234.

André, G. & Aubry, S. [1980] "Analyticity breaking and Anderson localization in incommensurate lattices, *Ann. Isr. Phys. Soc.* **3**, 133-140.

Benettin, G., Galgani, L. & Strelcyn, J. M. [1976] "Kolmogorov entropy and numerical experiments," *Phys. Rev. A* **14**, 2338–2345.

Bezhaeva, Z. I. & Oseledets, V. I. [1996] "An example of a strange nonchaotic attractor," *Funct. Anal. Appl.* **30**, 223–229.

Bondeson, A., Ott, E. & Antonsen, T. M. [1985] "Quasiperiodically forced damped pendula and Schrödinger equation with quasiperiodic potentials : Implication of their equivalence," *Phys. Rev. Lett.* **55**, 2103–2106.

Brindley, J., & Kapitaniak, T. [1991] "Analytic predictors for strange non–chaotic attractors," *Phys. Lett. A* **155**, 361–364.

Cassol, A. S., Veiga, F. L. S. & Tragtenberg, M. H. R. [2000] "Strange nonchaotic attractor in a dynamical system under periodic forcing," LANL archives cond–mat0002329.

Chen, G., & Dong, X. [1998] *From Chaos to Order* (World Scientific, Singapore, 1998).

Crutchfield, J., Farmer, D. & Huberman, B. [1982] "Fluctuations and simple chaotic dynamics," *Phys. Rep.* **92**, 45–82.

Dawson, S., Grebogi, C., Sauer, T. & Yorke, J. A. [1994] "Obstructions to shadowing when Lyapunov exponent is near zero," *Phys. Rev. Lett.* **73**, 1927.

Ding, M., Grebogi, C. & Ott, E. [1989] "Dimensions of strange nonchaotic attractors," *Phys. Lett. A* **137**, 167–172.

Ding, W. X., Deutsch, H., Dinklage, A., & Wilke, C. [1997] "Observation of a strange nonchaotic attractor in a neon glow discharge," *Phys. Rev. E* **55**, 3769–3772.

Ditto, W. L., Spano, M. L., Savage, H. T., Rauseo, S. N., Heagy, J. & Ott, E. [1990] "Experimental observation of a strange nonchaotic attractor," *Phys. Rev. Lett.* **65**, 533–536.

Eckmann, J. P. [1981] "Roads to turbulence in dissipative dynamical systems," *Rev. Mod. Phys.* **53**, 643.

Eckmann, J. P., & Ruelle, D. [1985] "Ergodic theory of chaos and strange attractors," *Rev. Mod. Phys.* **57**, 617–656.

Feudel, U., Kurths, J. & Pikovsky, A. S. [1995] "Strange nonchaotic attractor in a quasiperiodically forced circle map," *Physica D* **88**, 176–186.

Grassberger, P., Badii, R. & Politi, A. [1988] "Scaling laws for invariant measures on hyperbolic & nonhyperbolic attractors, *J. Stat. Phys.* **51**, 135–178.

Grebogi, C., Ott, E., Pelikan, S. & Yorke, J. A. [1984] " Strange Attractors that are not chaotic," *Physica D* **13**, 261–268.

Grebogi, C., Ott, O., Romeiras, F. & Yorke, J. A.[1987] "Critical exponents for crisis–induced intermittancy," *Phys. Rev. A* **36**, 5365–5380.

Heagy, J. F., & Ditto, W. L. [1991] "Dynamics of a two–frequency parametrically driven Duffing oscillator," *J. Nonlinear Sci.* **1** ,423–455.

Heagy, J.F., & Hammel, S. M. [1994] "The birth of strange nonchaotic attractors," *Physica D* **70**, 140–153.

Huang, W., Ding, W. X., Feng, D. L. & Yu, C. X. [1994] "Estimation of Lyapunov–exponent spectrum of plasma chaos," *Phys. Rev. E* **50**, 1062–1069.

Kaneko, K. [1984] "Oscillation & doubling of torus," *Prog. Theor. Phys.* **72**, 202–215.

Kaplan, J. L. & Yorke, J. A. [1979] "Preturbulence: a regime observed in fluid flow model of Lorenz," *Comm. Math. Phys.* **67**, 93–108.

Keller, G. [1996] "A note on strange nonchaotic attractors," *Fund. Math.* **151**, 139–148.

Ketoja, J. A., & Satija, I. I. [1997] "Harper equation, the dissipative standard map and strange nonchaotic attractors: Relationship between an eigenvalue problem and iterated maps," *Physica D* **109**, 70–80.

Kostelich, E. J., Kan, I., Grebogi, C., Ott, E. & Yorke, J. A. [1997] "Unstable dimension variability: A source of nonhyperbolicity in chaotic systems," *Physica D* **109**, 81–90.

Kuptsov, P. V., [1998] "Critical Dynamics of Pitch-Fork Bifurcation in a System Driven by a Fractal Sequence," *Int. J. Bifurcation and Chaos* **8**, 741–746.

Lai, Y.C., [1996] "Transition from strange nonchaotic to strange chaotic attractors," *Phys. Rev. E* **53**, 57–65.

Liu, Z., & Zhu, Z. [1996] "Strange nonchaotic attractors from quasiperiodically forced Ueda's circuit," *Int. J. Bifurcation and Chaos* **6**, 1383–1388.

Lorenz, E. N., [1963] "Deterministic nonperiodic flow," *J. Atmos. Sci.* **20**, 130–141.

Mandell, A. J., & Selz, K. A. [1993] "Brain stem neuronal noise & neocortical 'Resonance'," *J. Stat. Phys.* **70**, 355–372.

Mehra, V., & Ramaswamy, R. [1996] "Maximal Lyapunov exponent at crises," *Phys. Rev. E* **53**, 3420–3424.

Negi, S. S., Prasad, A. & Ramaswamy, R. [2000] "Bifurcations and transitions in the quasiperiodically driven logistic map," *Physica D*, in press.

Negi, S. S., & Ramaswamy, R. [2000a] "A plethora of fractal nonchaotic attractors," preprint.

Negi, S. S., & Ramaswamy, R. [2000b] "On driven maps of Harper type," preprint.

Negi, S. S., & Ramaswamy, R. [2000c] "Critical states & fractal attractors in fractal tongues:

Localization in the Harper map," submitted.

Nishikawa, T., & Kaneko, K. [1996] "Fractalization of a torus as a strange nonchaotic attractor," *Phys. Rev. E* **54**, 6114–6124.

Ott, E. [1994] *Chaos in dynamical systems* (Cambridge University Press, Cambridge, UK).

Ott, E., & Sommerer, J. C.[1994] "Blowout bifurcations: the occurance of riddled basins and on–off intermittancy," *Phys. Lett. A* **188**, 39–47.

Pecora, L. M., & Carroll, T. L. [1990] "Synchronization in Chaotic Systems," *Phys. Rev. Lett.* **64**, 821–824.

Pikovsky, A. S., & Feudel, U. [1995] "Characterizing strange nonchaotic attractors," *Chaos* **5**, 253–260.

Pikovsky, A., Zaks, M. A., Feudel U., & Kurths, J. [1995] "Singular continuous spectra in dissipative dynamics," *Phys. Rev. E* **52**, 285–296.

Pikovsky, A. S., & U. Feudel, [1997] "Strange nonchaotic attractors in autonomous and periodically driven systems," *Phys. Rev. E* **56**, 7320–7321.

Pomeau, Y., & Manneville, P. [1980] "Intermittent transition to turbulence in dissipative dynamical systems, *Comm. Math. Phys.* **74**, 189–197.

Prasad, A., Mehra, V. & Ramaswamy, R.[1997] "Intermittency route to Strange Nonchaotic Attractors," *Phys. Rev. Lett.* **79**, 4127–4130.

Prasad, A., Mehra, V. & Ramaswamy, R. [1998] "Strange Nonchaotic Attractors in the quasiperiodically forced Logistic Map," *Phys. Rev. E* **57**, 1576–1584.

Prasad, A., & Ramaswamy, R. [1998] "Finite-time Lyapunov exponents of strange nonchaotic attractors," in *Nonlinear Dynamics: Integrability & Chaos*, edited by M Daniel, R Sahadevan & K Tamizhmani (Narosa, New Delhi) pp. 227–34.

Prasad, A., & Ramaswamy, R. [1999] "Characteristic distributions of finite-time Lyapunov exponents," *Phys. Rev. E* **60**, 2761–2766.

Prasad, A., Ramaswamy, R., Satija, I. & Shah, N. [1999] "Collision & symmetry–breaking in the transition to strange nonchaotic attractors," *Phys. Rev. Lett.* **83**, 4530–4533.

Prasad, A., Negi, S. S., Datta, S. & Ramaswamy, R. [2000] "Symmetries of finite time Lyapunov exponents," preprint.

Prasad, A., & Ramaswamy, R. [2000] "Can strange nonchaotic attractors be created through stochastic driving?," *Proc. Ind. Natl. Sci. Acad.* in press.

Rajasekhar, S.[1995] "Controlling of chaotic motion by chaos and noise signals in a logistic map and Bonhoeffer – van der Pol oscillator," *Phys. Rev. E* **51**, 775–778.

Ramaswamy, R.[1997] "Synchronization of strange nonchaotic attractors," *Phys. Rev. E* **56**, 7294–7296.

Romeiras, F. J., Bondeson, A., Ott, E., Antonsen Jr., T. M. & Grebogi, C. [1987] "Quasiperiodically forced dynamical systems with strange nonchaotic attractors, *Physica D* **26**, 277–294.

Ruelle, D., & Takens, F. [1971] "On the nature of turbulence," *Comm. Math. Phys.* **20**, 167–192.

Schroer, C. G., Ott, E. & Yorke, J. A. [1998] "Effect of noise on nonhyperbolic chaotic attractors," *Phys. Rev. Lett.* **81**, 1397–1400.

Shinbrot, T. [1995] "Progress in the control chaos," *Adv. Physics* **44**, 73–111.

Shuai, J. M & Wong, K. W. [1998] "Nonchaotic attractors with highly fluctuating finite–time Lyapunov exponents," *Phys. Rev. E* **57**, 5332–5336.

Shuai, J. M & Wong, K. W. [1999] "Simple approach to the creation of a strange nonchaotic attractor in any chaotic system," *Phys. Rev. E* **59**, 5338–5343.

Sosnovtseva, O., Feudel, U., Kurths, J. & Pikovsky, A. [1996] "Multiband strange nonchaotic attractors in quasiperiodically forced systems," *Phys. Lett. A* **218**, 255–267.

Venkatesan, A., & Lakshmanan, M. [1998] " Different routes to chaos via strange nonchaotic attractors in a quasiperiodically forced system," *Phys. Rev. E* **58**, 3008–3016.

Venkatesan, A., Lakshmanan, M., Prasad, A. & Ramaswamy, R. [2000] "Intermittency transitions to strange nonchaotic attractors in a quasiperiodically driven Duffing oscillator," *Phys. Rev. E* **61**, 3641–3651.

Yalçinkaya, T., & Lai, Y. C. [1996] "Blowout bifurcation route to strange nonchaotic attractors," *Phys. Rev. Lett.* **77**, 5039–5042.

Yalçinkaya, T., & Lai, Y. C. [1997] "Bifurcation to strange nonchaotic attractors," *Phys. Rev. E* **56**, 1623–1630.

Yang, T., & Bilimgut, K. [1997] "Experimental results of strange nonchaotic phenomenon in a second order quasi–periodically forced electronic circuit," *Phys. Lett. A* **236**, 494–504.

Witt, A., Feudel, U. & Pikovsky, A. S. [1997] "Birth of strange nonchaotic attractors due to interior crises," *Physica D* **109**, 180–190.

Wolf, A., Swift, J. B., Swinney, H. L. & Vastano, J. A. [1985] "Determining Lyapunov exponents from a time series," *Physica D* **16**, 285–317.

Zhu Z., & Liu, Z. [1997] "Strange nonchaotic attractors of Chua's circuit with quasiperiodic excitation," *Int. J. Bifurcation and Chaos* **7**, 227–238.

Zhou, T., Moss, F. & Bulsara, A. [1992] "Observation of strange nonchaotic attractor in a multistable potential," *Phys. Rev. A* **45**, 5394–5400.

Zhou, C., & Chen T. [1997] "Robust communication via synchronization between nonchaotic strange attractors", *Europhys. Lett.* **38**, 261–265.

Figure Captions

Fig. 1. The trajectory of a strange (a) nonchaotic and (b) chaotic attractor of Eq. (1) at $q_2 = 0.88$ and $q_2 = 0.38$ respectively. The other parameters are $k = \beta = 2$ and $q_1 = 2.768$. In c) and d), trajectories with two different initial conditions, x (dotted line) and x' (solid line) are shown for the attractors of a) and b) respectively.

Fig. 2 Schematic phase diagram for the forced logistic map, Eq. (14). The rescaled parameter ϵ' is defined as $\epsilon' = \epsilon/(4/\alpha - 1)$. P and C correspond to regions of torus and chaotic attractors. SNAs are mainly found in the shaded region along the boundary of P and C (marked S). The actual boundaries separating the different regions are more convoluted than shown, and regions of SNA and chaotic attractors are interwoven in a complicated manner. Intermittent SNAs are found on the edge of the C_2 region marked I, while the left boundary of C_2 has only fractalized SNAs. Along the boundary of C_1, SNAs formed by either the torus collision mechanism or fractalization can be found. This phase diagram is discussed in detail in Prasad *et al.*[1997, 1998].

Fig. 3. Density of finite–time Lyapunov exponents $P(1000, \lambda)$ for an intermittent SNA in the forced logistic map, Eq. (14) at $\alpha = 3.84549, \epsilon' = 0.073$. See Prasad and Ramaswamy [1998] for details.

Fig. 4. Plot of the phase sensitivity function Γ_N vs N in the logistic map, Eq. (14) along $\epsilon' = 1$, for the fractalized SNA at $\alpha = 2.7$ (solid line) and a nearby torus at $\alpha = 2.5$ (dotted line). The exponent was found to be ≈ 2.35 (the dashed line is a least–squares fit). Note that this numerical value of the exponent depends on the system and its parameters; but in all cases Γ_N diverges with N.

Fig. 5. $|T(\Omega, N)|^2$, the singular–continuous spectral component, plotted versus N for an intermittent SNA at $\epsilon' = 1$, $\alpha = 3.405805$ in the quasiperiodic logistic map, Eq. (14) for $\Omega \equiv \omega/4$. The measured slope, here ≈ 1.75 (dashed line), changes with parameters and from system to system.

Fig. 6. A sequence of torus attractors and the corresponding SNA at the transition (indicated by the vertical dotted line in Fig. 7) in different scenarios. In the forced logistic map, Eq. (14) with $\epsilon' = 0.3$, a) the tori at $\alpha = 3.487$ and b) the SNA at $\alpha = 3.489$ following the Heagy–Hammel route. The dashed line in a) and b) is the unstable period-1 repeller. Fractalization at $\epsilon' = 1$ c) the torus attractor at $\alpha = 2.6$ and d) the SNA at $\alpha = 2.7$. The intermittency transition at $\epsilon' = 1$, with e) the wrinkled torus at $\alpha = 3.405809$ and f) the SNA at $\alpha = 3.405808$. The example of the blowout bifurcation route to SNA is in the mapping Eq. (28) with parameter $b = 1$; g) the torus at $a = 1.9$ and h) the SNA at $a = 2.1$. The homoclinic collision route in the Harper map, Eq. (9) with parameters $E = 0$, ω the golden mean ratio; i) the invariant curves at $\alpha = 0.8$, below the transition, and j) the SNA at $\alpha = 1.08$. In (i) and (j), for convenience the variable plotted on the ordinate is $\tanh(x)$, which has the range [-1,1] rather than x which has the range $(-\infty, \infty)$.

Fig. 7. Plot of the largest Lyapunov exponent (left) and its variance (right) across the transition from tori to SNAs, corresponding to the plots shown in Fig. 6. The vertical line in each panel is drawn at the parameter value corresponding to the transition. (a) and (b) are for the Heagy-Hammel route in the logistic map, Eq. (14) at the transition at $\alpha_c = 3.48779\ldots$ for $\epsilon' = 0.3$; (c) and (d) are for the fractalization route, also in the same system, with $\alpha_c = 2.6526\ldots$ at $\epsilon' = 1$; (e) and (f) are for the intermittent transition at $\alpha_c = 3.405808806\ldots$, $\epsilon' = 1$ and (g) and (h) are for the blowout bifurcation route in the mapping, Eq. (28), with $\alpha_c = 2.0$ at $b = 1$.

Fig. 8. The transition from SNA to a chaotic attractor in the logistic map, Eq. (14) along $\epsilon' = 0.3$. (a) The Lyapunov exponent across the transition, and (b) its fluctuations, σ, calculated from 50 samples, each of total length 10^7 iterations.

Fig. 9. The symmetry breaking in the blowout route to SNA. The return map for the stretch–exponents (a) at the bifurcation point in the mapping, Eq. (28), with $\alpha_c = 2.0$ at $b = 1$, and (b) at $\alpha = 2.01$, when the dynamics is on a SNA and the symmetry is clearly broken.

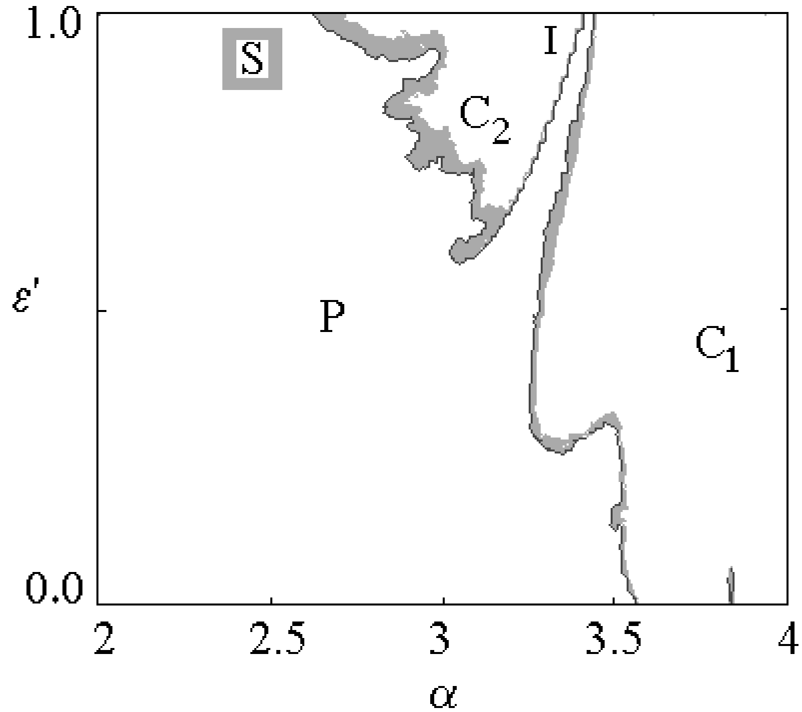
1.0
0.0
S
I
C2
P
C1
ε'
2
2.5
3
3.5
4
α

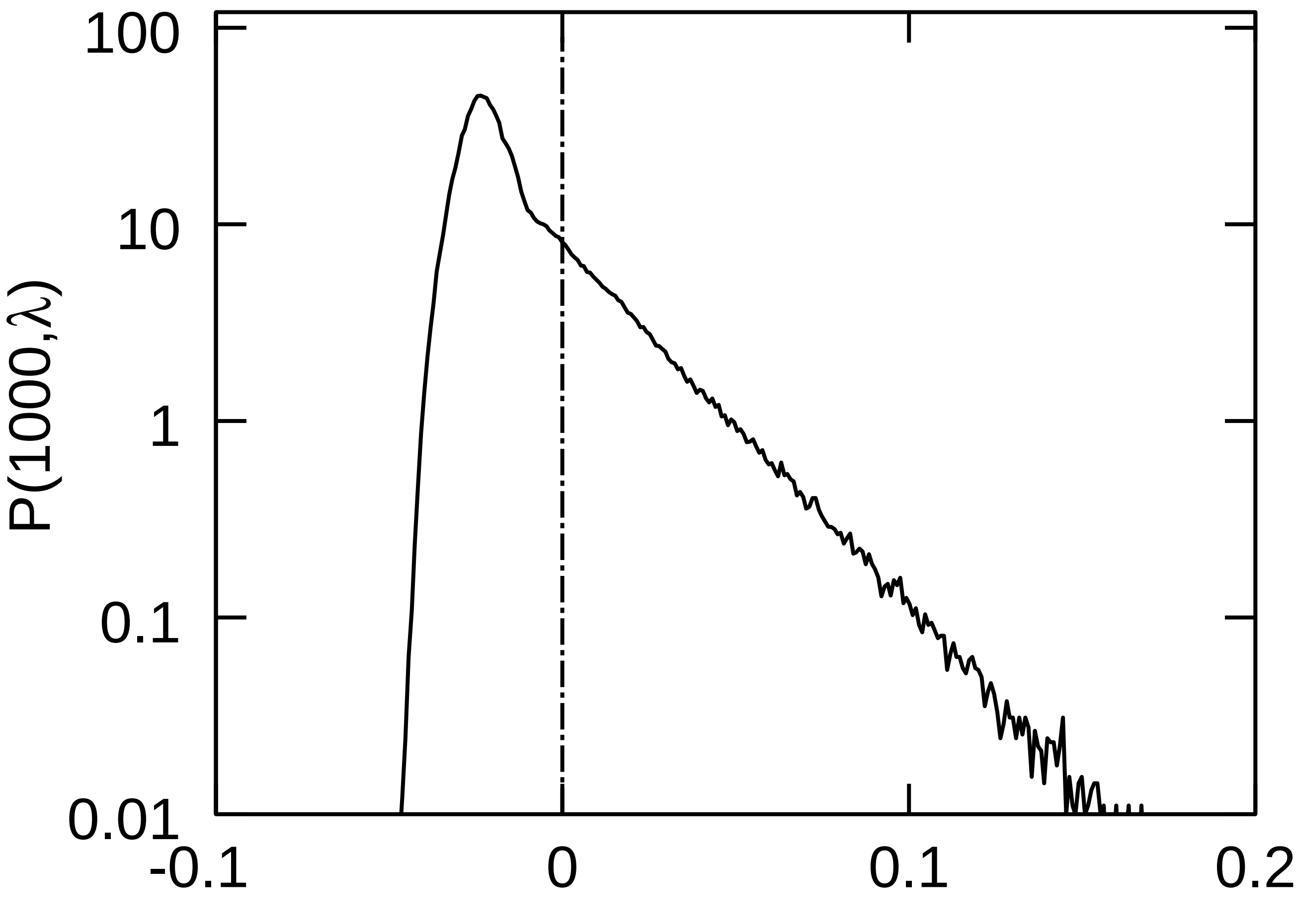

100
10
1
0.1
0.01
-0.1
0
0.1
0.2
P(1000,λ)
λ

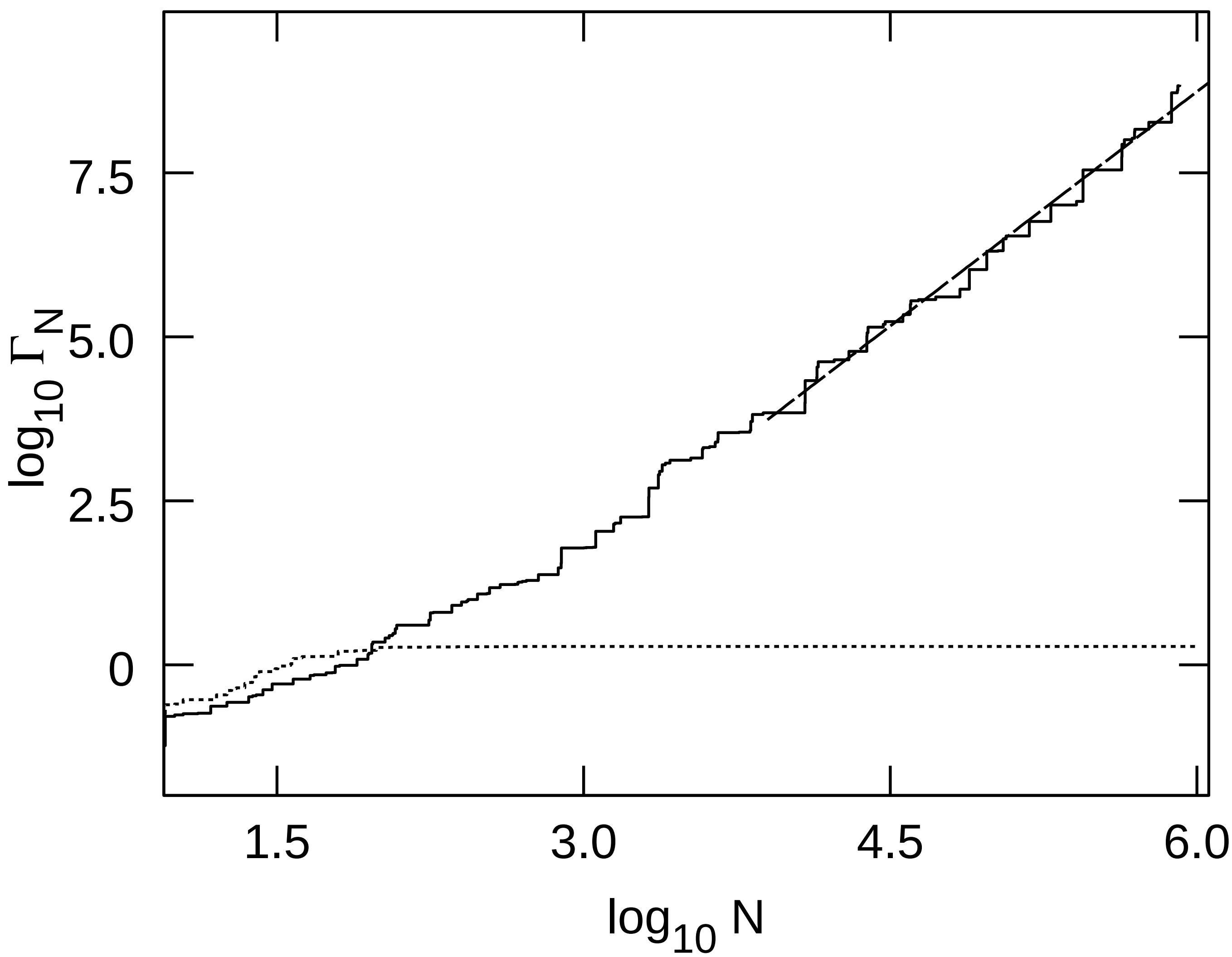

7.5
5.0
2.5
0
1.5
3.0
4.5
6.0
$\log_{10} \Gamma_N$
$\log_{10}$ N

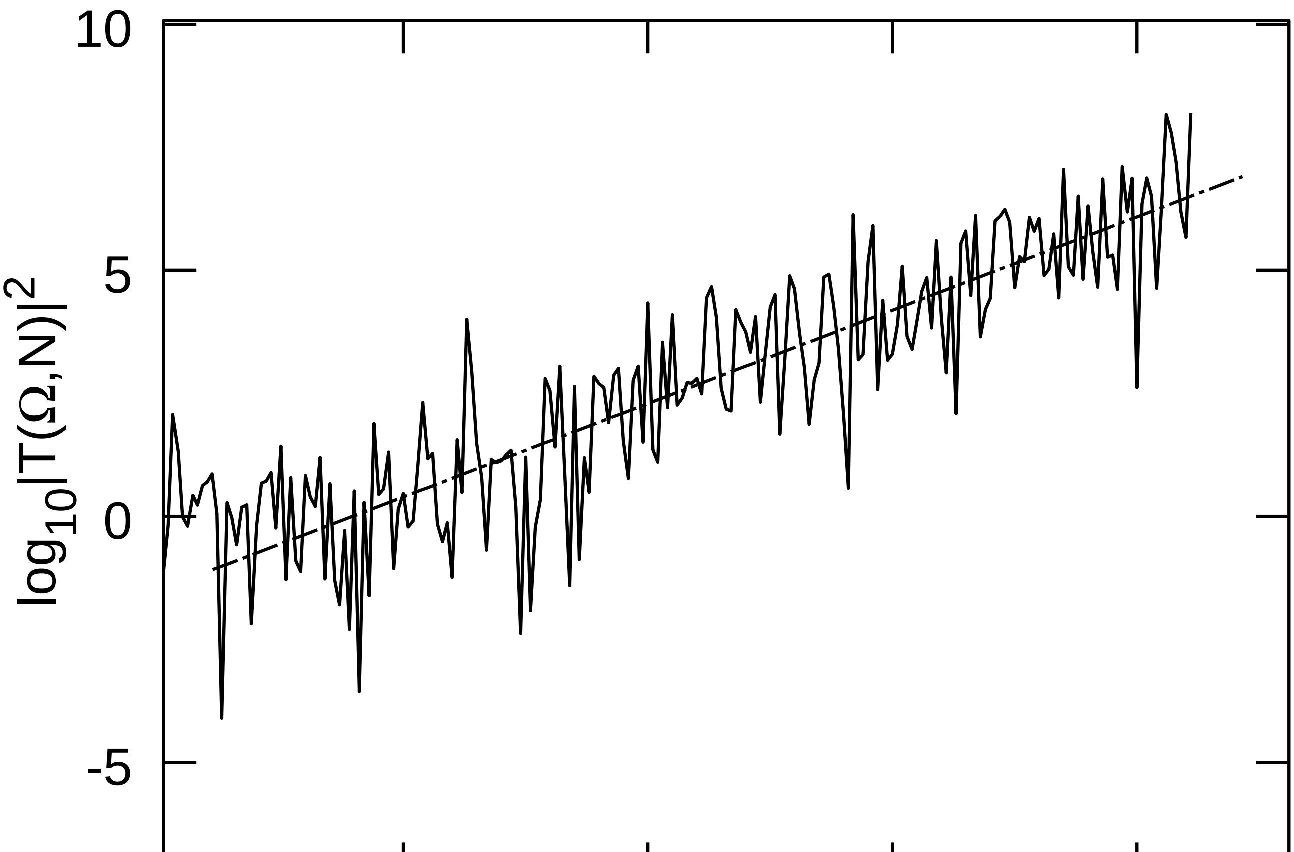

10
5
0
-5
3
4
5
6
$\log_{10} N$
$\log_{10}|T(\Omega,N)|^2$

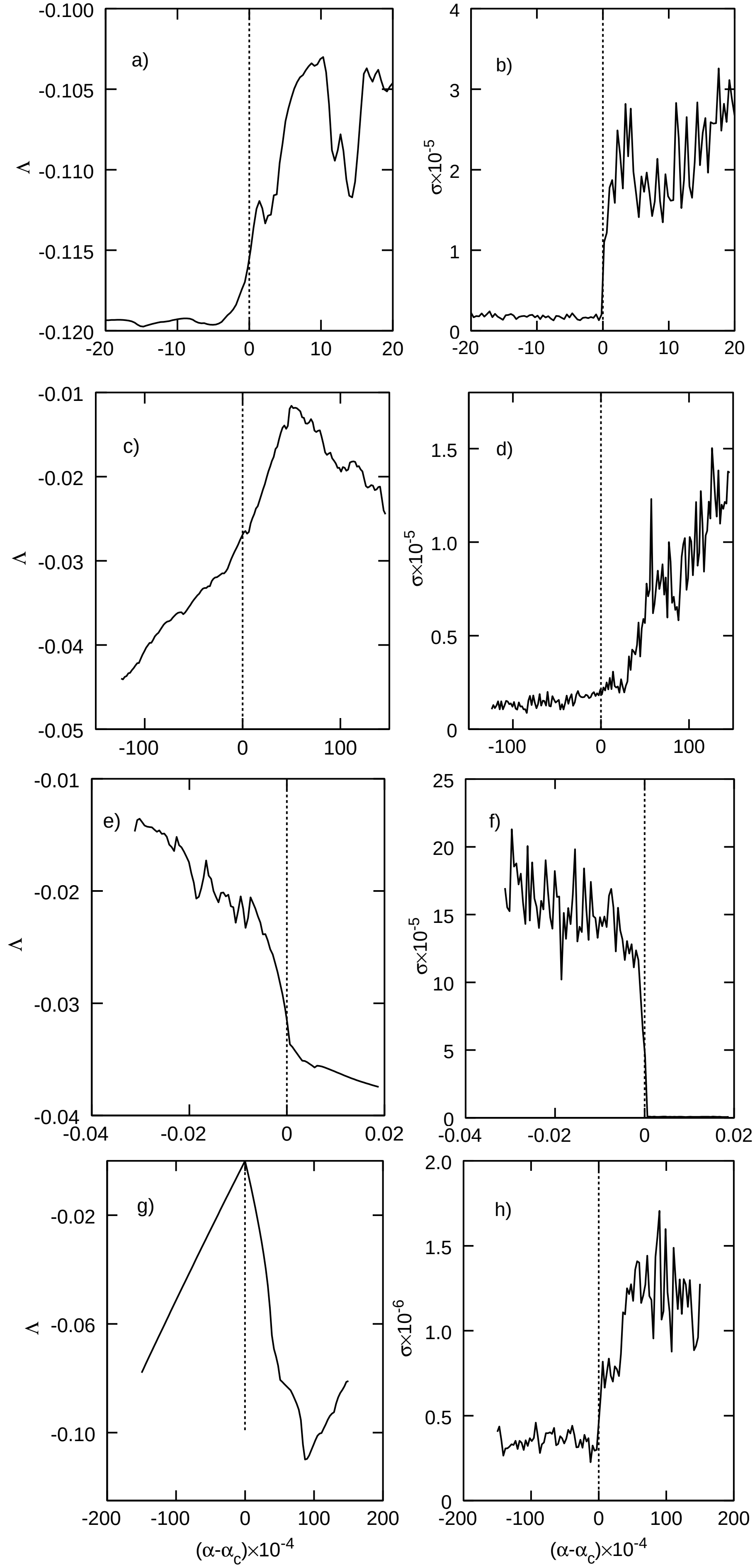
a)
b)
c)
d)
e)
f)
g)
h)
Λ
σ×10^-5
σ×10^-6
-0.100
-0.105
-0.110
-0.115
-0.120
-20
-10
0
10
20
4
3
2
1
-0.01
-0.02
-0.03
-0.04
-0.05
-100
100
1.5
1.0
0.5
25
15
5
-0.02
-0.06
-0.10
-200
200
2.0
(α-α_c)×10^-4
(α-α_c)×10^-4

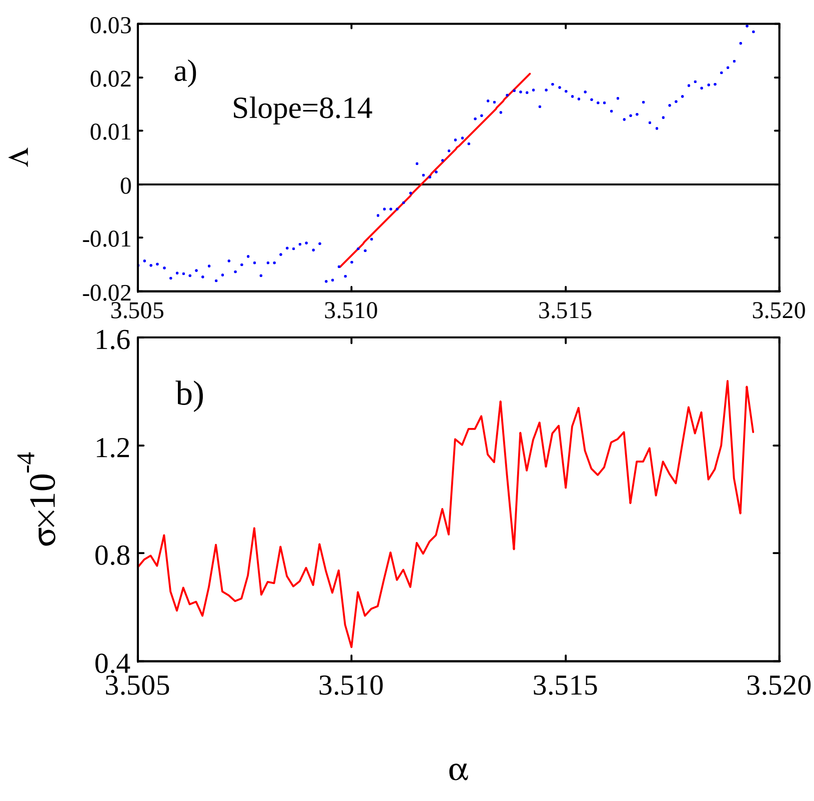
a)
Slope=8.14
Λ
0.03
0.02
0.01
0
-0.01
-0.02
3.505
3.510
3.515
3.520
b)
σ×10^-4
1.6
1.2
0.8
0.4
3.505
3.510
3.515
3.520
α